

Article

# C/EBP $\beta$ Is a Transcriptional Regulator of Wee1 at the G<sub>2</sub>/M Phase of the Cell Cycle

Ji Hae Lee <sup>1,†</sup>, Jee Young Sung <sup>2,†</sup>, Eun Kyung Choi <sup>1,†</sup>, Hyun-Kyoung Yoon <sup>1</sup>, Bo Ram Kang <sup>1</sup> , Eun Kyung Hong <sup>3</sup>, Byung-Kiu Park <sup>2</sup>, Yong-Nyun Kim <sup>1</sup>, Seung Bae Rho <sup>1</sup> and Kyungsil Yoon <sup>1,\*</sup>

<sup>1</sup> Division of Translational Science, Research Institute, National Cancer Center, Goyang, Gyeonggido 411-769, Korea; jhlee5@ncc.re.kr (J.H.L.); museonthat@naver.com (E.K.C.); 74670@ncc.re.kr (H.-K.Y.); sirosama@hanmail.net (B.R.K.); ynk@ncc.re.kr (Y.-N.K.); sbrho@ncc.re.kr (S.B.R.)

<sup>2</sup> Division of Clinical Research, Research Institute, National Cancer Center, Goyang, Gyeonggido 411-769, Korea; sungjy@ncc.re.kr (J.Y.S.); bkpark@ncc.re.kr (B.-K.P.)

<sup>3</sup> Department of Pathology, National Cancer Center, Goyang, Gyeonggido 411-769, Korea; hongek@ncc.re.kr

\* Correspondence: kyoons@ncc.re.kr; Tel.: +1-82-31-920-2325; Fax: +1-82-31-920-2337

† These authors contributed equally to this paper.

Received: 18 January 2019; Accepted: 9 February 2019; Published: 11 February 2019



**Abstract:** The CCAAT/enhancer-binding protein  $\beta$  (C/EBP $\beta$ ) is a transcription factor that regulates cellular proliferation, differentiation, apoptosis and tumorigenesis. Although the pro-oncogenic roles of C/EBP $\beta$  have been implicated in various human cancers, how it contributes to tumorigenesis or tumor progression has not been determined. Immunohistochemistry with human non-small cell lung cancer (NSCLC) tissues revealed that higher levels of C/EBP $\beta$  protein were expressed compared to normal lung tissues. Knockdown of C/EBP $\beta$  by siRNA reduced the proliferative capacity of NSCLC cells by delaying the G<sub>2</sub>/M transition in the cell cycle. In C/EBP $\beta$ -knockdown cells, a prolonged increase in phosphorylation of cyclin dependent kinase 1 at tyrosine 15 (Y15-pCDK1) was displayed with simultaneously increased Wee1 and decreased Cdc25B expression. Chromatin immunoprecipitation (ChIP) analysis showed that C/EBP $\beta$  bound to distal promoter regions of *WEE1* and repressed *WEE1* transcription through its interaction with histone deacetylase 2. Treatment of C/EBP $\beta$ -knockdown cells with a Wee1 inhibitor induced a decrease in Y15-pCDK1 and recovered cells from G<sub>2</sub>/M arrest. In the xenograft tumors, the depletion of C/EBP $\beta$  significantly reduced tumor growth. Taken together, these results indicate that Wee1 is a novel transcription target of C/EBP $\beta$  that is required for the G<sub>2</sub>/M phase of cell cycle progression, ultimately regulating proliferation of NSCLC cells.

**Keywords:** cell cycle; lung cancer; C/EBP $\beta$ ; G<sub>2</sub>/M arrest; Wee1; Y15-pCDK1

## 1. Introduction

CCAAT/enhancer-binding protein  $\beta$  (C/EBP $\beta$ ) is a member of the basic leucine zipper (bZIP) class of transcription factors and is involved in regulating cell growth, differentiation, inflammation, metabolism, survival, and tumorigenesis [1–5]. The growth-regulatory function of C/EBP $\beta$  has been reported to inhibit [6,7] or promote [8–11] cell proliferation, both in normal [6,8–10] and cancer cells [7,9,11]. For example, in C/EBP $\beta$  knock-out mice, hyperproliferation of epidermal keratinocytes was observed [6], but cell proliferation of B lymphocytes and gastric mucosa was decreased [8,9]. Thus, it is important to investigate how the function of C/EBP $\beta$  is determined in the cellular context and to determine what elicits these opposite growth responses including upstream regulators and downstream effectors.

C/EBP $\beta$  was shown to be required for carcinogen-induced mouse skin tumorigenesis by regulating p53-induced apoptosis upon carcinogen treatment [12,13], even though it induced

differentiation of epidermal keratinocytes in normal physiology [6]. Reduced skin-tumorigenic potential was also observed in v-Ha-Ras transgenic mice when C/EBP $\beta$  was deficient, thereby suggesting C/EBP $\beta$  plays an oncogenic role in the downstream Ras signaling pathway [12]. The analysis of gene expression patterns of human cancers revealed that C/EBP $\beta$  is involved in cyclin D1-induced oncogenic signature [14]. Furthermore, increased expression of C/EBP $\beta$  and its oncogenic roles have been reported in breast, ovarian, colorectal, renal, and gastric cancers [15–20]. However, its detailed mechanism and function are yet to be determined.

The cell cycle is tightly controlled to prevent incorrect DNA replication or immature cell division that induces genomic instability, a hallmark of cancer [21]. Cell cycle progression is proceeded by cyclin-dependent kinases (CDKs) and their partner cyclins which regulate the activity of CDKs. Cyclin D-CDK4 and cyclin D-CDK6 play a role in G<sub>1</sub> progression [22], and cyclin E-CDK2, cyclin A-CDK2, and Cyclin B-CDK1 regulate the G<sub>1</sub>/S transition, S phase progression, and the G<sub>2</sub>/M transition, respectively [23–25]. CDK activity is also regulated by activating phosphorylation by CDK-activating kinase [26] and inhibitory phosphorylation by Wee1 and Myt1 [27]. Dephosphorylation of inhibitory phosphorylation by Cdc25 activates CDK activity and enables cells to continue cell cycle progression [27]. CDK inhibitors including the INK4 family that consists of p15, p16, p18, and p19 [28], and the Cip/Kip family comprising p21, p27 and p57 [29–31] also control CDK activity. In human cancers, mutation or dysregulated expression of genes involved in cell cycle regulation are frequently observed [21], which is attributed to accelerated cancer cell growth, leading to more malignant progression.

Lung cancer is the leading cause of cancer death worldwide and is also the most frequently diagnosed [32]. Non-small cell lung cancers (NSCLCs) account for approximately 85% of human lung cancer, and among them, lung adenocarcinoma and lung squamous cell carcinoma are most prevalent [33]. In NSCLC, altered regulation of cell cycle proteins including inactivation of p16, reduced expression of p27 and Rb, and overexpression of cyclin D were reported [21]. In addition, high expression of cyclin E and cyclin A, and low expression of Rb were correlated with unfavorable prognosis in NSCLC patients [34]. These observations imply that dysregulation of cell cycle is critical to lung cancer development, and altered cell cycle regulatory proteins could be important therapeutic targets or prognostic markers.

Lung cancer is a genetically heterogeneous disease, and in lung adenocarcinoma, K-RAS and epidermal growth factor receptor (EGFR) are most commonly activated by mutations [33]. Both oncogene products potentiate cell cycle progression upon mitogenic signaling, resulting in more aggressive phenotypes. As C/EBP $\beta$  has been reported to mediate several oncogenic signaling pathways, including receptor tyrosine kinases or activated Ras [12,35], and the growth-regulatory function of C/EBP $\beta$  in lung cancer has not been fully defined, we investigated the role of C/EBP $\beta$  in human NSCLCs.

In this paper, we report that C/EBP $\beta$  is frequently overexpressed in lung cancer tissues compared with normal lungs tissues, and regulates cell proliferation by mediating cell cycle progression at the G<sub>2</sub>/M phase in NSCLC cells.

## 2. Materials and Methods

### 2.1. Cell Culture and Reagents

A549, Calu-6, NCI-H1299, NCI-H1703, NCI-H1975, NCI-H23, NCI-H460, HCC2279, NCI-H522, A427, Calu-3, NCI-H358, HCC827 and BEAS2B were obtained from the American Type Culture Collection (Rockville, MD, USA). HCC95 and HCC1588 were obtained from the Korean Cell Line Bank (Seoul, Korea), and Normal human bronchial epithelial (NHBE) purchased from Lonza. A549, Calu-6, NCI-H1299, NCI-H1703, NCI-H1975, NCI-H23, NCI-H460, HCC2279, NCI-H522, NCI-H358, HCC827, HCC95, HCC1588, and BEAS2B were cultured with RPMI1640. Calu-3 and A427 were cultured with Dulbecco's modified eagle medium (DMEM). NHBE was cultured with bronchial epithelial cell growth

medium (BEGM) BulletKit (Lonza, Walkersville, MD, USA). All cell lines were maintained in media supplemented with 10% fetal bovine serum (FBS) and  $1 \times$  penicillin-streptomycin, and cultured under standard conditions at 37 °C in a humidified atmosphere of 95% air and 5% CO<sub>2</sub>. Stock solutions of the Wee1 inhibitor MK-1775 (Selleck Chemicals, Houston, TX, USA) were dissolved in dimethyl sulfoxide (DMSO) and added to the media at the indicated concentrations (100 nM). Doxycycline (D9891) was purchased from Sigma-Aldrich (St. Louis, MO, USA). Matrigel was purchased from Corning Inc (Corning, NY, USA).

## 2.2. siRNA Transfection and Generation of Conditional Knockdown Cell Lines

Cells were seeded in 6-well culture plates at a density of  $2 \times 10^5$  cells per well, and grown for 16 h before transfection with 20 nM of small interfering RNA (siRNA) for 48 h. The sequences of the CCAAT/enhancer binding protein  $\beta$  (C/EBP $\beta$ ) siRNA are as follows: siC/EBP $\beta$  #1, 5'-CCTCGCAGGTCAAGAGCAA-3'; siC/EBP $\beta$  #2, 5'-CCAAGAAGACCGTGGACAA-3'. SiRNA duplexes were transfected using Lipofectamine 2000 (Invitrogen, Waltham, MA, USA) following the manufacturer's protocol. To generate doxycycline-inducible C/EBP $\beta$ -knockdown cell lines, the C/EBP $\beta$  target sequences were cloned into the Tet-pLKO-Puro plasmid (Addgene plasmid #21915). The Tet-on-shC/EBP $\beta$  target sequence is 5'-CACCCCTGCGGAACCTTGTTCAA-3'. To induce C/EBP $\beta$ -knockdown, doxycycline (100 ng/mL) was added.

## 2.3. Cell Proliferation Assay

Cells were plated in triplicate at 10% confluence in 24-well culture plates and transfected with negative control siRNA (siNC) or C/EBP $\beta$  siRNA (siC/EBP $\beta$ ) at a final concentration of 20 nM. Cells were harvested and counted using a Coulter counter (Beckman Coulter, Brea, CA, USA) in 24 h intervals. An IncuCyte live-cell imaging system (Essen Bioscience, Ann Arbor, MI, USA) was used to measure the proliferation of Tet-on-shC/EBP $\beta$  or shNC cells using the cell confluence approach.

## 2.4. Live/Dead Cell Staining

Cells were stained using LIVE/DEAD™ Viability/Cytotoxicity Kit (Thermo Scientific, Rockford, IL, USA) following the manufacturer's protocol. Images were obtained by an Operetta High Content Screening (HCS) System (PerkinElmer, Waltham, MA, USA) and analysis was performed using Harmony 3.5.2 software (PerkinElmer).

## 2.5. Cell Cycle Analysis

For thymidine double block [36], cells were seeded at  $2 \times 10^5$  cells per well in 6-well culture plates and treated with thymidine at 2 mM for 14 h. Cells were then washed, supplemented with normal media for 12 h, and treated with 2 mM thymidine for another 14 h. The cells were harvested at 2 h intervals up to 16 h and 26 h after release. Afterward, cells were harvested and fixed in 75% (*v/v*) cold ethanol at −20 °C for at least 2 h. The fixed cells were collected by centrifugation and resuspended in propidium iodide (PI) Staining Buffer (Sigma, St. Louis, MO, USA) to stain DNA and analyzed for DNA content on a flow cytometry (FACSCaliber; Becton Dickinson, Franklin Lakes, NJ, USA).

## 2.6. Live Cell Fluorescence Imaging for Analysis of Motosis

A549 cells were seeded in 12-well culture plates and transfected with negative control siNC or siC/EBP $\beta$ . After 24 h, cells were stained with NucBlue® live reagent (Hoechst 33342 dye, Thermo Scientific, Rockford, IL, USA) for 20 min following manufacturer's protocol, then replaced with fresh culture medium. Images were taken by Operetta High Content Screening (HCS) System (PerkinElmer, Waltham, MA, USA) every 10 min for 48 h under 200 $\times$  magnification.

### 2.7. Western Blot Analysis

Whole-cell lysates were prepared in radioimmunoprecipitation assay (RIPA) buffer, supplemented with protease inhibitor cocktail, phosphatase inhibitor (Calbiochem, San Diego, CA, USA), phenylmethylsulfonyl fluoride (PMSF), and dithiothreitol (DTT). Protein concentrations were determined using a micro bicinchoninic acid (BCA) protein assay kit (Thermo Scientific, Rockford, IL, USA). Equal amounts of protein were separated by 6–12% Sodium dodecyl sulphate-polyacrylamide gel electrophoresis (SDS-PAGE) and transferred to a polyvinylidene difluoride (PVDF) membrane (BioRad, Hercules, CA, USA) using a wet transfer device (BioRad, Hercules, CA, USA). The following antibodies were used in this study: C/EBP $\beta$  (sc-7962), MAD2 (sc-6329), and  $\beta$ -actin (sc-477778) (all obtained from SantaCruz Biotechnology, Santa Cruz, CA, USA); anti-Cdc2/Cdk1 (06-923), phospho-Cdk1 (Tyr15) (#9111), Cdc25B (#9525), Wee1 (#4936), and Cdc25A (#3652) (all obtained from Cell Signaling Technology Beverly, MA, USA); and anti-CyclinB1 (05-373) and Cdc25C (05-507) (all obtained from Millipore, Bedford, MA, USA).

### 2.8. Quantitative Real-Time PCR

Total RNA was prepared by using Trizol (Ambion, Life Technologies, Carlsbad, CA, USA) and cDNA was synthesized using Moloney murine leukemia virus (M-MLV) reverse transcriptase (Invitrogen, Waltham, MA, USA). Real-time polymerase chain reaction (PCR) was performed using LightCycler<sup>®</sup> 96 Real-Time PCR System (Roche, Basel, Switzerland). Each reaction was performed with 10 ng cDNA by using SYBR Green. Primer sequences used for PCR were as follows: Wee1, (F: 5'-TTCAATGAGGAGACTTGCCTG-3' and R: 5'-ACAACAACAATCTGAGGTGCC-3'); Cdc25B, (F: 5'-GTGAGGAAGTTTCAGAACAGTCCG-3' and R: 5'-TGGGAGGCTTGTCGCATTTG-3'), and GAPDH, (F: 5'-TGATGACATCAAGGTGGTGAAG-3' and R: 5'-TCCTTGGAGGCCATGTGGGCCAT-3'). PCR reactions were performed as follows: 95 °C denaturation for 5 min, followed by 40 cycles at 94 °C for 10 s, 60 °C for 10 s, 72 °C for 10 s, followed by a 9-min extension at 72 °C. For displaying PCR products on agarose gel, PCR cycle was reduced to 30 cycles.

### 2.9. Chromatin Immunoprecipitation

The chromatin immunoprecipitation (ChIP) assay was performed using the EZ-ChIP assay (Upstate Biotechnology, Lake Placid, NY, USA) following the manufacturer's protocol. Briefly, formaldehyde was added at a final concentration of 1% directly to cell culture media. Fixation proceeded at RT for 10 min and was stopped by the addition of glycine to a final concentration of 0.125 M. The cells were collected by centrifugation and rinsed in cold phosphate-buffered saline (PBS). The cell pellets were resuspended in hypotonic buffer containing 0.5 mM PMSF, protease inhibitor cocktail, and incubated on ice for 15 min. The nuclei were collected by micro-centrifugation and then resuspended in SDS lysis buffer (1% SDS, 10 mM EDTA, 50 mM Tris-HCl (pH 8.1), 0.5 mM PMSF, and protease inhibitor cocktail). The samples were sonicated to an average length of 300–500 bp with a S220 Focused-ultrasonicator (Covaris, Woburn, MA, USA). Chromatin immunoprecipitation was performed with anti-C/EBP $\beta$  (sc-150X, SantaCruz Biotechnology, Santa Cruz, CA, USA) or HDAC2 (sc-9959X, SantaCruz Biotechnology, Santa Cruz, CA, USA) and protein G agarose. ChIP products were eluted and DNA was recovered from reverse crosslinking and purification. C/EBP $\beta$  binding to specific sites on the *Wee1* promoter was analyzed by quantitative real-time PCR (qRT-PCR). Primers for PCR analysis were follows: R1 (F: 5'-CAGTCTAGTTGTGGAGAGGCA-3' and R: 5'-CCTGCCACTCCTGATGACAAA-3'); R2 (F: 5'-CAGTGTGTGCTTTACTCAGAGGAG-3' and R: 5'-CTCCAGCAACCAGCACTGT-3'); R3 (F: 5'-TCAAAGTGCAAGGCTCATGT-3' and R: 5'-TTTGCAGAATCCACATGCTT-3'); R4 (F: 5'-TGCTGATGAACATGCCGTGA-3' and R: 5'-CTGCCATTTGGCCTCAGGAA-3'); *GAPDH* exon (F: 5'-TCTATAAATTGAGCCCGCAGC-3' and R: 5'-GCGACGCAAAGAAGATGC-3').

### 2.10. Luciferase Reporter Assay

The constructs of *Wee1* promoter region were cloned into pGL3-promoter firefly luciferase vector (Promega, Madison, WI, USA), which were named R3 (−4932 to −4679), and R2 (−4543 to −4380). *C/EBPβ* and HDAC2 cDNA clones purchased from OriGene were sub-cloned into pcDNA3.1 vector (Invitrogen, Waltham, MA, USA). Cells were seeded in 24-well plates and co-transfected with reporter vectors and pcDNA3.1 or pcDNA3.1-*C/EBPβ* and/or pcDNA3.1-HDAC2 as indicated using Lipofectamine 2000 (Invitrogen). After 48 h, cells were harvested. Firefly luciferase activities were determined using the Luciferase assay system kit (Promega, Madison, WI, USA), as described by the manufacturer, with a luminescence plate reader (VICTOR™ X, PerkinElmer, Waltham, MA, USA). The firefly luciferase activity was normalized for transfection efficiency with protein measurement using a BCA protein assay. Data are expressed as relative luciferase activity/μg protein.

### 2.11. Immunoprecipitation

Cells were lysed in cell lysis buffer (20 mM Tris-HCl pH8.0, 150 mM NaCl, 1 mM Na<sub>2</sub>EDTA, 1 mM EGTA, 1% Triton, 2.5 mM sodium pyrophosphate, and 1 mM β-glycerophosphate). Each cell lysate (1 mg) was incubated with *C/EBPβ* monoclonal antibody (Santacruz Biotechnology, Santa Cruz, CA, USA) overnight at 4 °C. Following incubation, protein was immunoprecipitated using protein G agarose beads (GE Healthcare, Chicago, IL, USA) for 2 h at 4 °C with gentle rotation. The immunoprecipitates were washed three times with lysis buffer and boiled in 20 μL of 1× SDS sample buffer for 5 min at 95 °C. After centrifugation, the supernatant was analyzed using Western blot.

### 2.12. Xenograft Mouse Model and siRNA Delivery

A549 ( $5 \times 10^6$ ) cells were suspended in 100 μL PBS and mixed with 50 μL Matrigel (Corning Inc.). The mixtures were implanted subcutaneously into 6-week-old athymic nude mice. When the tumor size reached 60 to 80 mm<sup>3</sup>, the dilute siRNA solution in sterile PBS (50 μL) was directly injected into the xenograft tumor via electroporation using NEPA21 Super Electroporator (Nepa gene Co., Chiba, Japan). The tumor size was monitored every 7 days up to 7 weeks. Tumor diameters were measured twice a week and the volume was calculated with the following formula:  $V \text{ (mm}^3\text{)} = \text{longest diameter} \times \text{shortest diameter}^2 / 2$ .

### 2.13. Immunohistochemical Staining for Xenograft Tumor

Xenograft tumors were removed and fixed in 10% formalin, embedded in paraffin, and cut into 4-μm sections. The sections were used for immunohistochemical staining performed with the automated instrument Discovery XT (Ventana Medical Systems, Inc., Tucson, AZ, USA) using anti-*C/EBPβ* (sc-150, Santacruz Biotechnology, Santa Cruz, CA, USA), anti-*Wee1* (ab37597), *Cdc25B* (ab70927), phospho-*Cdk1*(Tyr15) (ab133463), anti-*Ki67* (ab15580) (all from Abcam, Cambridge, UK), and cleaved caspase3 (#9661, Cell signaling Technology Beverly, MA, USA).

### 2.14. Immunohistochemical Staining for Lung Cancer Tissue Microarray

Lung tissue arrays [CCN5, Human, Normal lung (59 adjacent normal lung tissues matching CC5, 1 carbon); CC5, Human, Lung cancer (59 NSCLC tissues, 1 carbon); CCA4 Human, Lung cancer-metastasis-normal (36 NSCLCs, 1 missing NSCLC, 2 small cell lung cancers (SCLCs), 1 malignant mesothelioma; 9 metastatic tissues matching 9 among 36 NSCLCs, 1 metastatic tissue matching 1 among 2 SCLCs; 9 normal lung tissues matching 9 among 36 NSCLC, 1 carbon] were purchased from Superbiochips Laboratories (Seoul, Korea) [37]. Total number of tissues on 3 microarrays was 68 for adjacent normal lung tissues, 95 for NSCLC tissues and 9 for metastatic tissues from 95 patients. Each array contained 59 sections of 4 μm thickness obtained by surgical resection and one carbon for orientation. The sections were used for immunohistochemical staining performed with the Ventana BenchMark XT Staining systems (Ventana Medical Systems, Inc.) using *C/EBPβ* antibody (1:30, sc-150 Santacruz Biotechnology, Santa

Cruz, CA, USA) and the UltraView Universal DAB detection kit (Ventana Medical Systems, Inc.). Parallel sections incubated with normal IgG antibody instead of primary antibodies were used for negative controls. The stainings were scored from 0 to 4 based on the intensity and proportion of positive staining in a tissue field. Stained tissue arrays were reviewed by two experienced medical pathologists. To obtain representative images, slides were scanned by the Aperio ScanScope scanner (Aperio Technologies, Vista, CA, USA) and images were captured using Aperio ImageScope software.

### 2.15. Statistical Analysis

All data points represent average values and standard deviation (SD) or standard error (SE) obtained from three independent experiments performed in triplicate. Comparison between two groups was performed using Student's *t*-test. The relationship between C/EBP $\beta$  expression and clinicopathologic characteristics was analyzed using the Student's *t*-test. Statistical significance was defined as a *p* value < 0.05. For survival analysis, Kaplan–Meier Plotter [38] was used to investigate the association of C/EBP $\beta$  mRNA expression in overall survival and post-progression survival in lung cancer patients.

## 3. Results

### 3.1. Levels of C/EBP $\beta$ Protein in Human Lung Cancer Tissues Were Elevated

To explore the clinical significance of C/EBP $\beta$  in lung cancer, we examined the expression of C/EBP $\beta$  in patient-derived lung cancer tissue microarrays. Lung cancer tissues and adjacent normal lung tissue obtained from 95 patients were immunohistochemically stained for C/EBP $\beta$ . Representative pictures of C/EBP $\beta$  staining results with varying intensities (0 to 4) are shown in Figure 1A. As shown in Figure 1B and Table 1, the proportion of normal lung tissues with positive C/EBP $\beta$  staining was only 30.9%, whereas positive C/EBP $\beta$  staining increased up to 67.3% in the primary lung cancer tissues, including 29.4% of strong staining intensity (score 2–4). Scoring of C/EBP $\beta$  staining in each NSCLC subtype is listed in Figure S1A. Tumor samples from metastatic patients tended to display strong staining for C/EBP $\beta$  (score 2–3, 55.5%), and positive C/EBP $\beta$  staining of metastatic tissues was significantly higher than that of normal lung tissues (Figure 1B). Immunohistochemical analyses of primary NSCLC tissues showed that C/EBP $\beta$  expression was already enhanced from the early stages of lung cancer but there were no significant differences among different clinical stages, tumor, node, metastasis (TNM) stage, age, or sex (Table 2). A significant increase in C/EBP $\beta$  positive staining was observed in squamous cell carcinoma and other types of NSCLCs compared with lung adenocarcinoma. Using a public database, we also analyzed gene alteration status of *C/EBPB* in lung adenocarcinoma and lung squamous cell carcinoma, the most common subtypes of non-small cell lung cancers (NSCLCs). The *C/EBPB* gene was amplified by 1.22% and 1.57% and deleted by 0.1% and 0.17% in lung adenocarcinoma and lung squamous cell carcinoma, respectively, indicating that alteration of the *C/EBPB* gene is not frequent (Figure S1B). An association between clinical outcomes of lung cancer patients and C/EBP $\beta$  expression was examined using the Kaplan–Meier Plotter [38]. This revealed that the levels of C/EBP $\beta$  mRNA were inversely correlated with the overall survival of patients with lung cancers, adenocarcinomas, and squamous cell carcinomas (Figure 1C and Figure S2A). Additionally, increased expression of C/EBP $\beta$  mRNA was associated with poor post-progression survival in all lung cancer and adenocarcinoma patients (Figure S2A,B). All these data indicate that the expression of C/EBP $\beta$  is upregulated at the protein levels, which is a functional moiety, in human lung cancer and possibly correlated with clinical outcome of patients.

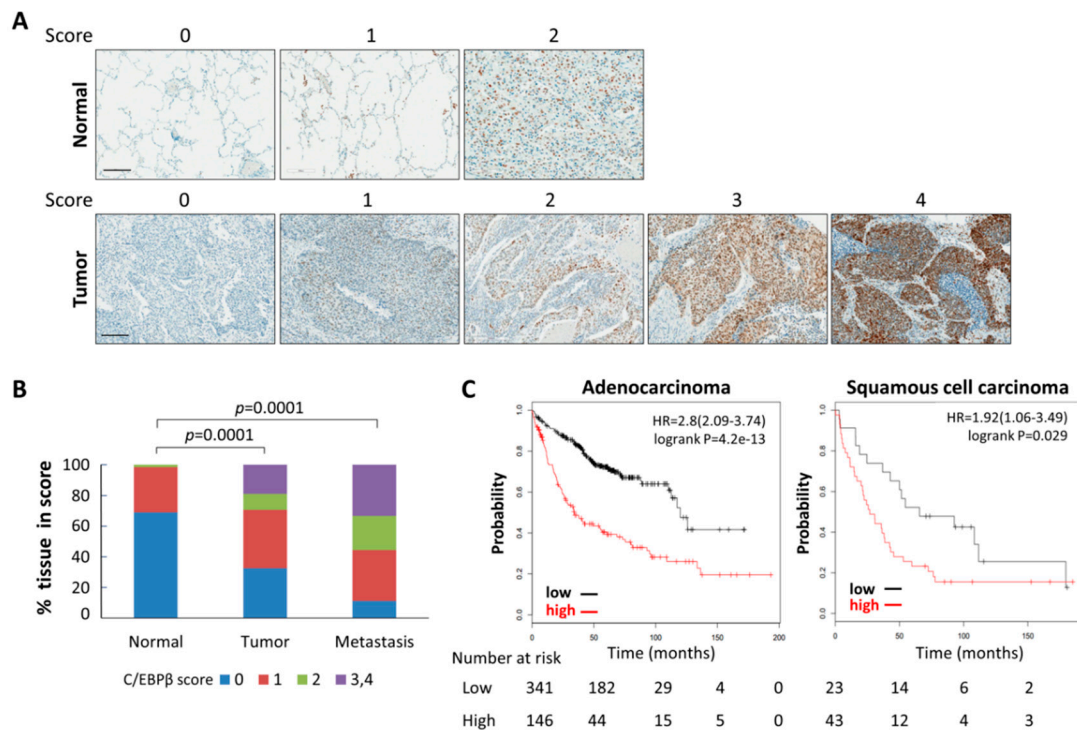


**Figure 1.** CCAAT/enhancer-binding protein  $\beta$  (C/EBP $\beta$ ) expression in human lung cancer tissues. (A) Patients-derived lung cancer tissue arrays were examined for C/EBP $\beta$  expression using the immunoperoxidase method. Staining results were graded according to the intensity and proportion of positive area. Images were captured at a magnification of 200X by using the Aperio ImageScope software. Scale bars: 200  $\mu$ m. (B) The histogram represents the percentage of the immunohistochemistry (IHC) score for C/EBP $\beta$  in 68 normal tissues, 95 primary, and 9 metastatic tumor tissues. The statistical significance was determined using the *t*-test,  $p < 0.05$ . (C) The association between C/EBP $\beta$  mRNA expression and overall survival of adenocarcinoma (whole dataset) and squamous cell carcinoma patients (GSE37745) was analyzed using the Kaplan–Meier Plotter. Hazard ratio (HR) significance was found with log-rank tests.

**Table 1.** Immunohistochemistry (IHC) scoring of C/EBP $\beta$ .

Score	Normal <i>n</i> (%)	Tumor <i>n</i> (%)	Metastasis <i>n</i> (%)
0	47 (69.1)	31 (32.6)	1 (11.1)
1	20 (29.4)	36 (37.9)	3 (33.3)
2	1 (1.5)	10 (10.5)	2 (22.2)
3	0 (0)	13 (13.7)	3 (33.3)
4	0 (0)	5 (5.3)	0 (0)
Total	68 (100)	95 (100)	9 (100)

**Table 2.** Summary of C/EBP $\beta$  expression and clinicopathological feature in the lung cancer patients.

	C/EBP $\beta$ Expression			<i>p</i> Value	
	Negative <i>n</i> (%)	Positive <i>n</i> (%)	Total <i>n</i> (%)		
<b>Sex</b>					
Male	23 (31)	52 (69)	75 (100)	0.4343	
Female	8 (40)	12 (60)	20 (100)		
<b>Age</b>					
≤57	11 (31)	24 (69)	35 (100)	0.8505	
>57	20 (33)	40 (67)	60 (100)		
<b>Clinical Stage</b>					
I	10 (27)	27 (73)	37 (100)	0.2305	
II	12 (32)	25 (68)	37 (100)		
III	9 (43)	12 (57)	21 (100)		
<b>N classification</b>					
0	15 (28)	38 (72)	53 (100)	0.2204	
1	8 (33)	16 (67)	24 (100)		
2	8 (44)	10 (66)	18 (100)		
<b>T classification</b>					
1	1 (13)	7 (87)	8 (100)	0.3039	
2	23 (33)	47 (67)	70 (100)		
3	5 (46)	6 (54)	11 (100)		
4	2 (33)	4 (67)	17 (100)		
<b>Histology</b>					
Adenocarcinoma	13 (46)	15 (54)	28 (100)	0.0180 *	0.0256 †
Squamous carcinoma	15 (31)	34 (69)	49 (100)		0.2941 #
Other NSCLC	3 (17)	15 (83)	18 (100)		

\* Adenocarcinoma vs. squamous cell carcinoma, † Adenocarcinoma vs. other NSCLC, # Squamous cell carcinoma vs. other NSCLC, \* † significantly different between two groups,  $p < 0.05$ . C/EBP $\beta$  staining was analyzed with 95 primary NSCLC tissues from 95 NSCLC patients.

### 3.2. Knockdown of C/EBP $\beta$ Inhibits Cell Proliferation Rates of NSCLC Cells

In this research, we measured the levels of C/EBP $\beta$  protein in normal human bronchiolar epithelial cells (NHBE), immortalized human bronchial epithelial cells (BEAS-2B), and various subtypes of NSCLC cell lines. Different subtypes of lung cancers are known to be distinct in origin and in disease progression [39]. NHBE cells expressed C/EBP $\beta$  protein in marginal amounts compared with BEAS-2B cells and NSCLC cell lines tested (Figure 2A). There was no significant association between C/EBP $\beta$  protein levels and specific NSCLC subtype.

K-Ras and EGFR is frequently activated by mutation and they are mutually exclusive in lung adenocarcinomas [33], and these oncogenes might act as upstream regulator of C/EBP $\beta$ . However, the levels of C/EBP $\beta$  protein were not very different among adenocarcinomas with mutant *K-RAS* (A549, H23, A427, NCI-H358), mutant *EGFR* (NCI-H1975, HCC827) and wild-type *K-RAS* and *EGFR* (NCI-H1703, NCI-H522, Calu-3) [40–44], even though A549 and H23 cells displayed relatively high levels of C/EBP $\beta$  (Figure 2A).

To examine the function of C/EBP $\beta$  in lung cancer cells, we knocked down C/EBP $\beta$  using two different siRNAs in NSCLC cell lines. Transfection of each siC/EBP $\beta$  dramatically suppressed proliferation of A549 cells with C/EBP $\beta$  down-regulation (Figure 2B). We also employed doxycycline-inducible shRNA targeting another sequence of C/EBP $\beta$  and observed that doxycycline treatment decreased C/EBP $\beta$  protein and cell proliferation (Figure 2C).

To exclude the possibility that retarded cell proliferation induced by C/EBP $\beta$ –knockdown was limited to A549 cells, we knocked down C/EBP $\beta$  in several NSCLC cell lines with decent levels of C/EBP $\beta$  protein (Figure 2D). Consistent with results shown in Figure 2B,C, cell proliferation

rates were significantly slower in siC/EBPβ-transfected NSCLC cells than in negative control-siRNA (siNC)-transfected cells (Figure 2E). Neither histological subtypes nor *EGFR* and *K-Ras* mutation status of the cell lines produced significant differences in the growth arrest induced by C/EBPβ-knockdown (Figure 2E). NSCLC subtypes and mutational status of *K-RAS* and *EGFR* in each cell line are listed in Table S1. Although C/EBPβ-knockdown attenuated cell proliferation in BEAS-2B cells, the degree of inhibition appeared minimal compared with NSCLC cell lines. These observations indicate that C/EBPβ is important for cell proliferation in NSCLC cells.

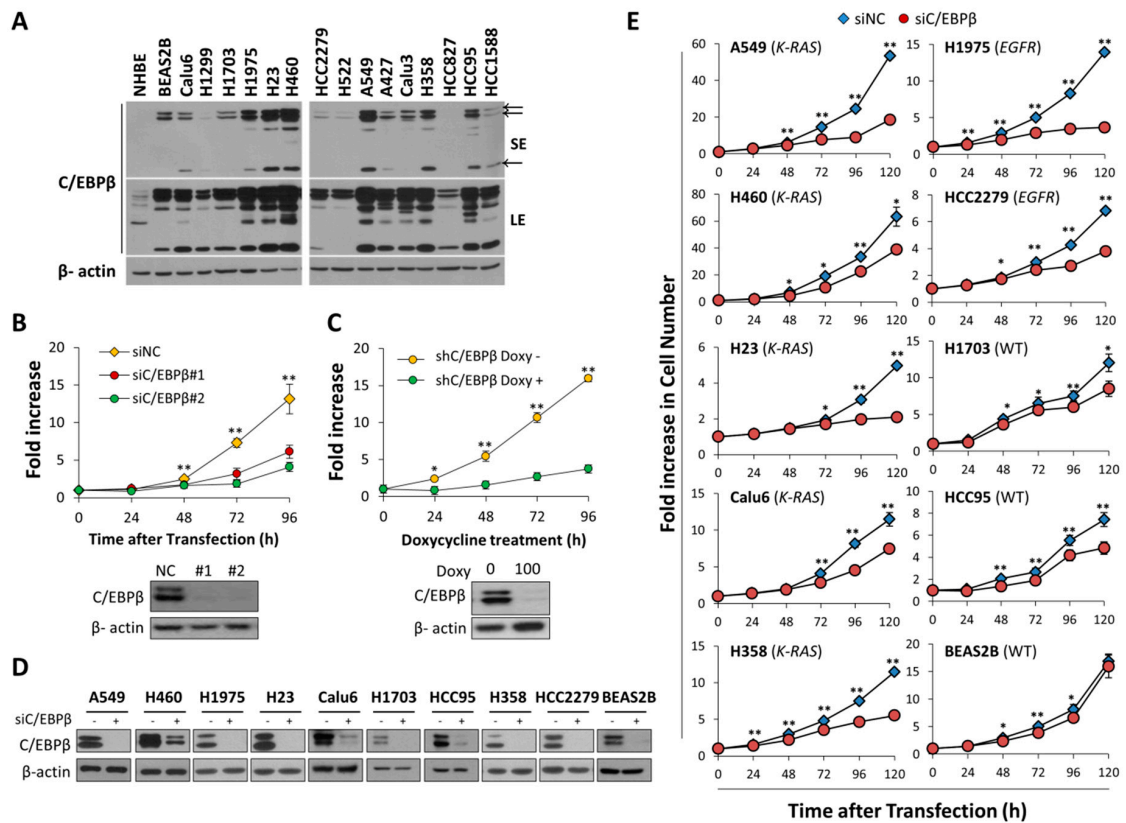


**Figure 2.** C/EBPβ promotes cell proliferation in various subtypes of non-small cell lung cancer (NSCLC) cell lines. (A) C/EBPβ protein levels in normal human bronchial epithelial cells (NHBE), immortalized human bronchial epithelial cells, BEAS-2B and various NSCLC cell lines were determined by Western blot analysis. Adenocarcinoma, A549, NCI-H1975, NCI-H23, NCI-H1703, NCI-H522, A427, Calu-3, NCI-H358; adeno-squamous cell carcinoma, HCC2279; squamous cell carcinoma, HCC95, HCC1588; large cell carcinoma, H460, NCI-H1299; anaplastic carcinoma, Calu-6. (B) Live cells of A549 transfected with si-Negative Control (siNC), siC/EBPβ #1, or siC/EBPβ #2 were counted with trypan blue staining at indicated times after transfection. Data are presented as fold increase. (C) Doxycycline-inducible shC/EBPβ cells using A549 were generated and treated with or without doxycycline (100 ng/mL). Using the InCuCyte live cell imaging system, proliferation cells was monitored and quantified by the percentage of cell confluence. (D) The protein levels of C/EBPβ were detected by Western blotting to check C/EBPβ-knockdown in each cell line. (E) Cell number of lung cancer cell lines transfected with siNC or siC/EBPβ (#1 + #2) was counted using a Coulter counter at intervals of 24 h up to 120 h after siRNA transfection. *K-RAS*: mutant *K-RAS*/wild-type *EGFR*, *EGFR*: wild-type *K-RAS*/mutant *EGFR*, WT: wild-type *K-RAS*/wild-type *EGFR*. Data are presented as mean ± standard deviation (SD). The statistical significance was determined using *t*-tests, \* *p* < 0.05, \*\* *p* < 0.01.

### 3.3. C/EBP $\beta$ -Knockdown Delayed G<sub>2</sub>/M Phase of the Cell Cycle Progression with Elevated Levels of Inhibitory Phosphorylation of CDK1

Next, we investigated whether inhibition of cell proliferation was due to increased cell death or inhibited cell cycle progression in the C/EBP $\beta$ -knockdown cells. There was little difference in cell death between control and C/EBP $\beta$ -knockdown cells (Figure 3A), indicating cell death was not involved in C/EBP $\beta$ -knockdown-induced inhibition of cell proliferation. We then examined the role of C/EBP $\beta$  in cell cycle regulation. We analyzed the cell cycle of C/EBP $\beta$ -knockdown cells by flow cytometry, which showed a significant decrease in the population of cells in the G<sub>0</sub>/G<sub>1</sub> and a simultaneous increase in the G<sub>2</sub>/M phase of the cell cycle compared with the control (Figure 3B). G<sub>2</sub>/M progression of the cell cycle is mainly regulated by cyclin B/CDK1 [45]. Activity of CDK1 is regulated by its phosphorylation. The Wee1 and Myt1 kinases phosphorylate CDK1 at tyrosine 15 (Tyr15), thereby inhibiting CDK1. Dephosphorylation of Tyr15 by cell division cycle 25 (Cdc25) phosphatase is required for the activation of CDK1 and further entry into mitosis [46–50]. Knockdown of C/EBP $\beta$  increased phosphorylation of CDK1 at the tyrosine 15 residue (Y15-pCDK1) with a simultaneous increase in the levels of Wee1 and cyclin B1 and a decrease in the levels of Cdc25B (Figure 3C). The expression of Cdc25A and Cdc25C remained unchanged between the groups. C/EBP $\beta$ -knockdown did not appear to affect the protein levels of Myt1 and mitotic arrest deficient 2 (Mad2), mitotic spindle checkpoint component [51]. Taken together, these data indicate that C/EBP $\beta$ -knockdown cells undergo a delay in the G<sub>2</sub>/M phase of the cell cycle, displaying elevated Y15-pCDK1 possibly due to increased Wee1 and decreased Cdc25B.

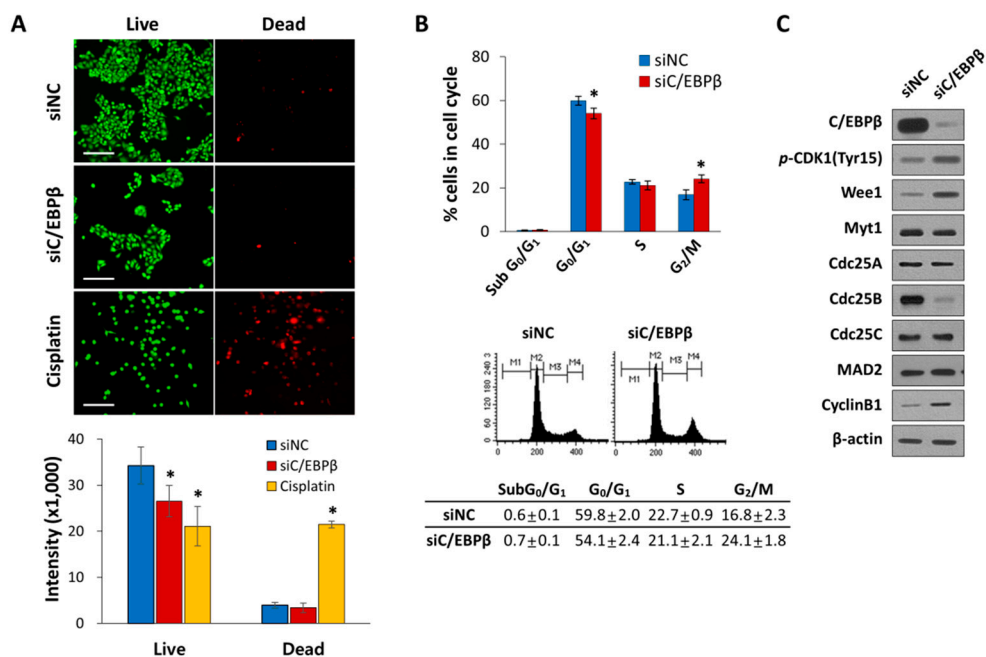


**Figure 3.** C/EBP $\beta$ -knockdown inhibits cell cycle progression. (A) A549 cells were transfected with siNC or siC/EBP $\beta$  and incubated for 48 h. As a positive control for cell death, cells were treated with 20 M cisplatin for 48 h. Live cells were stained with green calcein-AM, while dead cells were stained with red ethidium homodimer-1 (EthD-1). Cell images were taken at a magnification of 100X using an Operetta High Content Screening (HCS) System. Scale bar: 200  $\mu$ m. (B) A549 cells were transfected with control siRNA or C/EBP $\beta$  siRNA for 48 h. The cell cycle was analyzed by fluorescence-activated cell sorting (FACS) after DNA staining with propidium iodide (PI). M1: subG<sub>0</sub>/G<sub>1</sub>, M2: G<sub>0</sub>/G<sub>1</sub>, M3: S, and M4: G<sub>2</sub>/M phase. Percentage of cells in each cell cycle phase is shown as a bar graph. (C) Whole cell lysates were prepared 48 h after transfection and the levels of the G<sub>2</sub>/M cell cycle-related proteins in control or C/EBP $\beta$ -knockdown cells were analyzed by Western blotting.  $\beta$ -actin was used as a loading control. Data are presented as mean  $\pm$  SD. Statistical significance was determined using the *t*-test, \* *p* < 0.01.

In order to observe a temporal progression in the G<sub>2</sub>/M phase of the cell cycle, we synchronized cells at the G<sub>1</sub>/S boundary using thymidine double block methods [36], and released cells into the cell cycle by removing thymidine. Control cells progressed into the cell cycle and accumulated in the G<sub>2</sub>/M phase 6 h after release at the highest levels, and subsequently moved into the G<sub>1</sub> phase in just 2–4 h (Figure 4A,B). In contrast, C/EBPβ-knockdown cells reached the G<sub>2</sub>/M peak 8 h after release into the cell cycle, and stayed in the G<sub>2</sub>/M phase for much longer up to 16 h. Cell populations in the G<sub>2</sub>/M phase in an asynchronized condition (26 h) were significantly higher in C/EBPβ-knockdown cells compared with controls, consistent with results shown in Figure 3B. To determine the effect of C/EBPβ-knockdown on mitotic progression, we analyzed mitotic duration using time-lapse live cell imaging with nuclear Hoechst 33342 staining. As shown in Figure 4D, mitotic duration from nuclear envelope breakdown to anaphase onset [52] was not significantly different between control and C/EBPβ-knockdown cells, suggesting that a delay in the G<sub>2</sub>/M phase of the cell cycle progression displayed in C/EBPβ-knockdown cells was not due to a delay in the mitotic phase, but was rather due to prolonged stay in the G<sub>2</sub> phase of the cell cycle. To confirm a delay in the G<sub>2</sub>-M transition of C/EBPβ-knockdown cells, we analyzed mitotic cell populations using flow cytometry along with phospho-histone H3 (Ser10) and PI staining. Phosphorylation of histone H3 (Ser10) is essential for mitotic condensation and thus considered a mitotic marker [53]. As shown in Figure S3, more C/EBPβ-knockdown cells were accumulated in the G<sub>2</sub>/M phase than control cells, consistent with results in Figure 3B, but mitotic cells with positive phospho-histone H3 (Ser10) staining decreased significantly in C/EBPβ-knockdown cells. Combined with the live cell imaging results, C/EBPβ seem to be important in the G<sub>2</sub>/M transition of the cell cycle.

In the control cells, levels of Y15-pCDK1 started to decrease within 6 h and suddenly dropped 10 h after release when the most cells returned to the G<sub>1</sub> phase (Figure 4C). A timely and transient increase in Cdc25B protein levels was correlated with a decrease in Y15-pCDK1, which is an important event for mitotic entry. However, Y15-pCDK1 stayed at higher levels for a longer time with an increase in Wee1 and a delayed and attenuated Cdc25B induction in the C/EBPβ-knockdown cells compared with control cells (Figure 4C). Taken together, our data demonstrate that C/EBPβ is an important mediator at the G<sub>2</sub>/M phase of the cell cycle progression by regulating the expression of Wee1 and Cdc25B, which critically modulates Y15-pCDK1.

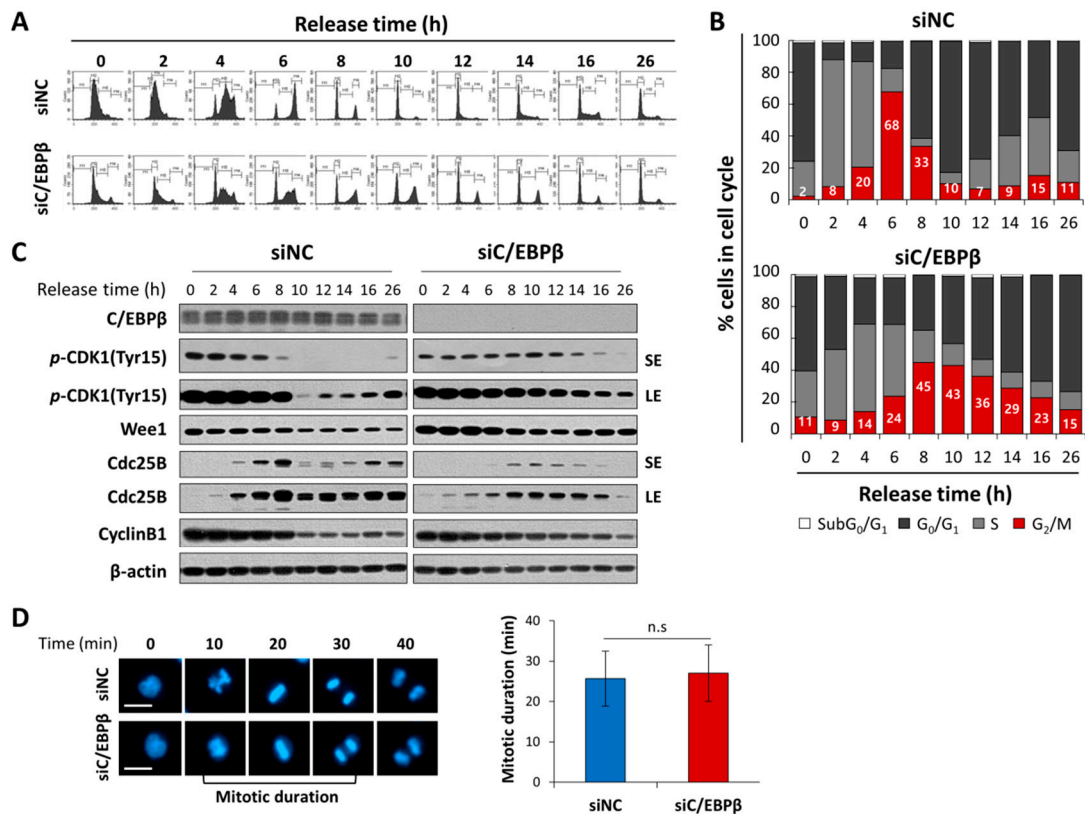


**Figure 4.** *C/EBPβ* knockdown delays  $G_2/M$ -cell cycle transition. (A) A time course study of the cell cycle analysis was performed in control or *C/EBPβ*-knockdown A549 cells. Cells were released from thymidine double block-induced  $G_1/S$  synchronization; and 0, 2, 4, 6, 8, 10, 12, 14, 16, and 26 h after releasing, cells were collected and stained with PI to measure DNA content using FACS. (B) The data are expressed as the percentage of cells in the sub $G_0/G_1$ ,  $G_0/G_1$ , S, and  $G_2/M$  phase at the indicated time points. (C) Whole cell lysates were prepared at the indicated times and Western blot analysis was performed for expression of proteins associated with the  $G_2/M$  transition (Y15-pCDK1, Wee1, Cdc25B and Cyclin B1). SE; short exposure, LE; long exposure. (D) Mitotic duration of control or *C/EBPβ*-knockdown A549 cells stained with NucBlue® was monitored by an Operetta High Content Screening (HCS) System. Representative images of siNC and siC/*EBPβ*-transfected cells from time lapse series were shown. Images were acquired every 10 min. Data are presented as mean  $\pm$  SD of mitotic duration in 30 cells in each group. Mitotic duration was measured from nuclear envelope breakdown (prometaphase) to anaphase onsets [52]. Statistical significance was determined using the *t*-test; n.s., not significant. Cell images were taken at a magnification of 200X using an Operetta High Content Screening (HCS) System. Scale bar: 20  $\mu$ m.

### 3.4. *C/EBPβ* Regulates *Wee1* Expression at the Transcription Levels

Next, we investigated if either *WEE1* or *CDC25B* was the transcription target of *C/EBPβ* playing a role in cell cycle regulation. As shown in Figure 5A, in *C/EBPβ*-knockdown cells, mRNA levels of *Wee1* and *Cdc25B* increased and decreased, respectively, correlated with their protein levels (Figure 5A). With our *C/EBPβ*-ChIP on chip data (unpublished data) and using a web-based tool for searching transcription factor binding sites, TFSEARCH [54], we predicted four putative *C/EBPβ* binding regions on the *WEE1* distal promoter, as shown in Figure 5B. We performed a *C/EBPβ*-ChIP assay and real-time PCR to verify that *C/EBPβ* bound to  $-4.7$  to  $-4.9$  kB (R3) and  $-4.4$  to  $-4.5$  kB (R2) upstream of the *Wee1* transcription start site (Figure 5C,F). However, we did not find any significant binding of *C/EBPβ* to the *CD25B* promoter based on our *C/EBPβ*-ChIP on chip data (unpublished data).

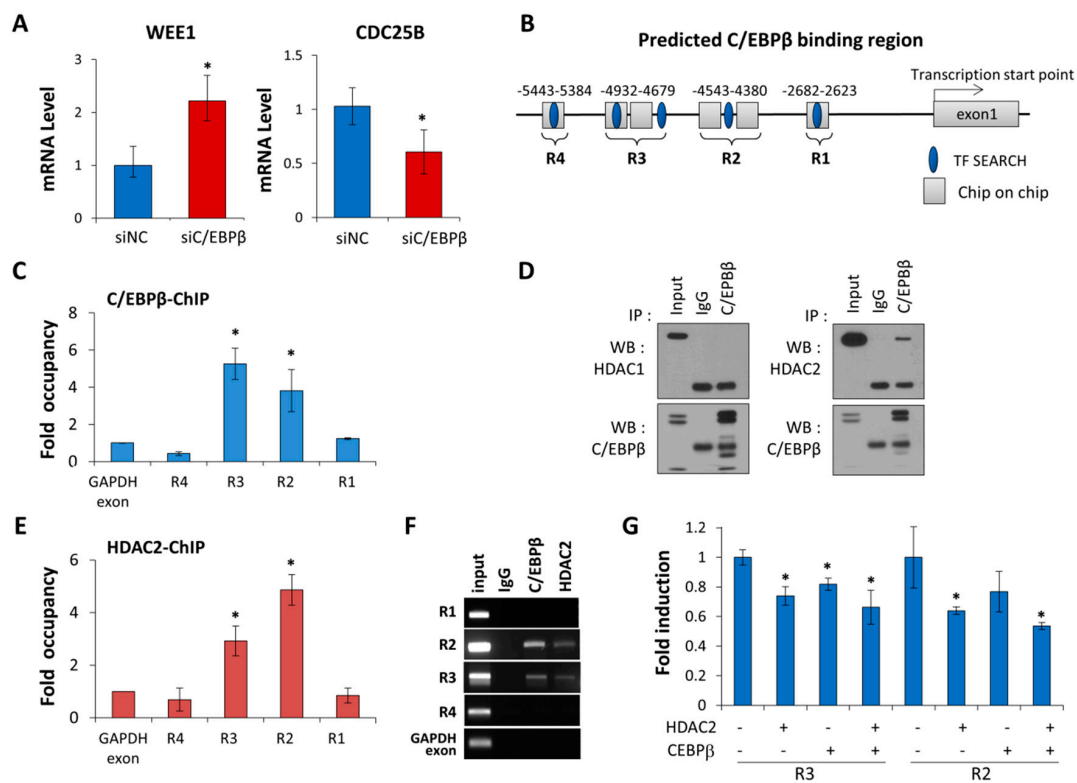


**Figure 5.** C/EBP $\beta$  regulates Wee1 expression at the transcription levels and interacts with HDAC2. (A) Quantitative real-time RT-PCR (qRT-PCR) was used to determine Wee1 and Cdc25B mRNA levels relative to the control gene GAPDH in C/EBP $\beta$ -knockdown A549 cells. Data are presented as mean  $\pm$  SD. (B) The position of the four predicted C/EBP $\beta$  binding sites in the WEE1 promoter are represented. C/EBP $\beta$ -ChIP on chip data and TFSEARCH based binding sites are indicated as a rectangle and an oval, respectively. The prediction of WEE1 promoter regions was based on NCBI accession number (NC\_000011.10, GRCh37.p11) (C) The C/EBP $\beta$ -ChIP assay followed by qRT-PCR on putative C/EBP $\beta$  binding regions on the WEE1 promoter was performed to determine endogenous C/EBP $\beta$  occupancy at the specified region. The fold enrichment of C/EBP $\beta$  occupancy over GAPDH exon (negative control) is shown. Data are presented as mean  $\pm$  SE. (D) A549 cell lysates were immunoprecipitated using anti-C/EBP $\beta$  antibodies. Immunocomplexes were analyzed by Western blot with either anti-HDAC1 or -HDAC2 antibodies. IgG was used as a negative control. (E) HDAC2-ChIP assay followed by qRT-PCR on putative C/EBP $\beta$  binding regions at the WEE1 promoter was performed. The fold enrichment of HDAC2 occupancy over GAPDH exon (negative control) is shown. Data are presented as mean  $\pm$  SE. (F) The C/EBP $\beta$ -ChIP or HDAC2-ChIP assay followed by PCR on putative C/EBP $\beta$  binding regions at the WEE1 promoter was performed. The PCR products resolved on 2% agarose gel were visualized. (G) A549 cells were co-transfected with a WEE1 promoter-luciferase construct containing R2, or R3 along with C/EBP $\beta$  and/or HDAC2, as indicated, for 48 h, and then luciferase activities were measured. Data are expressed as relative luciferase activity/ $\mu$ g protein standardized by a control pGL3-promoter vector. Data are presented as mean  $\pm$  SD. Statistical significance was determined using the *t*-test, \* *p* < 0.05.

C/EBP $\beta$  has been reported to interact with histone deacetylase1 (HDAC1) and repress the activation of the C/EBP $\alpha$  promoter [55]. Our data showed that C/EBP $\beta$  interacts with HDAC2, not with HDAC1 in A549 cells (Figure 5D). In addition, the HDAC2-ChIP assay revealed that HDAC2 also bound to the R2 and R3 regions (Figure 5E,F), suggesting that C/EBP $\beta$  recruits HDAC2 at the WEE1 distal promoter. To determine if C/EBP $\beta$  in conjunction with HDAC2 repressed WEE1 promoter activity, we constructed a promoter-reporter vector containing either the R2 or R3 region of the distal WEE1 promoter. Enforced expression of C/EBP $\beta$  or HDAC2 alone reduced WEE1 promoter-reporter

activity and C/EBPβ along with HDAC2 further decreased transcriptional activity of the *WEE1* promoter, indicating that C/EBPβ recruits HDAC2 to the *WEE1* promoter, negatively regulating *WEE1* transcription (Figure 5G). Taken together, we identified Wee1, a mitosis inhibitor, as a novel transcription target gene of C/EBPβ.

### 3.5. C/EBPβ-Knockdown Cells Treated with MK1775 Were Recovered from G<sub>2</sub>/M Delay

To confirm Wee1 plays an important role in a delay in the G<sub>2</sub>/M cell cycle shown in C/EBPβ deficiency, we examined whether the inhibition of Wee1 could release C/EBPβ-knockdown cells from the delay in the G<sub>2</sub>/M. Four hours after release into the cell cycle at the completion of the thymidine double block, cells were treated with a Wee1 inhibitor, MK1775, or DMSO. MK1775 treatment of control cells had little effect on cell cycle progression (Figure 6A,B). However, Wee1 inhibition of C/EBPβ-knockdown cells diminished accumulation of cell populations in the G<sub>2</sub>/M phase induced by C/EBPβ-deficiency (Figure 6A,B). More specifically, C/EBPβ-knockdown cells accumulated in the G<sub>2</sub>/M phase up to 10 h (62.2%) because of a delay in the G<sub>2</sub>/M phase and decreased to 43.6% at 12 h after release. However, upon MK-1775 treatment of C/EBPβ-knockdown cells, cell populations in the G<sub>2</sub>/M phase maximally reached up to 57.8% at 8 h, further progressed into the G<sub>0</sub>/G<sub>1</sub> and S phase, and then decreased to 44.9% and 22% at 10 and 12 h after release, respectively. Consistent with the results in Figures 3 and 4, compared with control cells, Y15-pCDK1 increased in the C/EBPβ-knockdown cells (Figure 6C). Treatment with MK1775 induced a rapid decrease in Y15-pCDK1 with little changes in total levels of CDK1. As MK1775 treatment rescued C/EBPβ-knockdown cells from the delay in the G<sub>2</sub>/M phase, we argue that increased Y15-pCDK1 by Wee1 is responsible for the delay in the G<sub>2</sub>/M phase with defective C/EBPβ function.

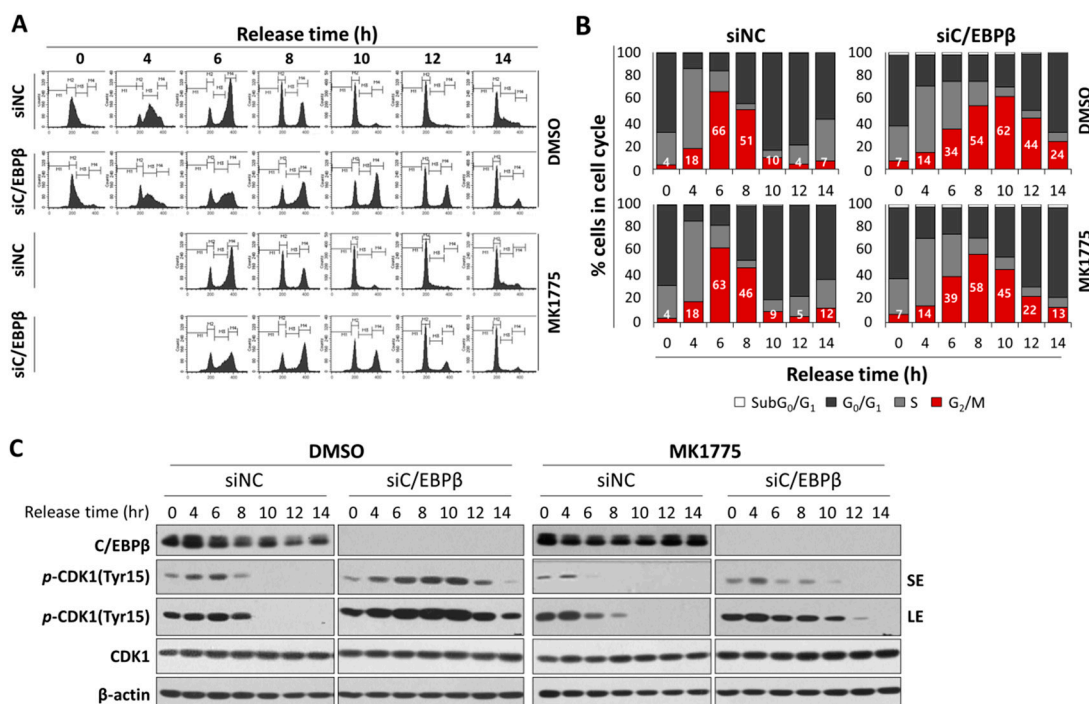


**Figure 6.** C/EBPβ knockdown cells treated with MK1775 recovered from the delay in the G<sub>2</sub>/M phase. (A,B) A549 cells transfected with siNC or siC/EBPβ were treated with either DMSO or MK1775 4 h after being released from thymidine double block. Cells were harvested for cell cycle analysis at different time points after release, and DNA contents with PI staining were analyzed using FACS. (C) Expression of cell cycle-associated proteins was analyzed in DMSO- or MK1775-treated control cells and C/EBPβ-knockdown cells. Percentage of cells in each cell cycle phase is shown as a bar graph. SE; short exposure, LE; long exposure.

### 3.6. C/EBP $\beta$ -Knockdown Inhibits Tumor Growth In Vivo

Since C/EBP $\beta$ -knockdown inhibits cell proliferation inducing a delay in the G<sub>2</sub>/M phase of the cell cycle, we tested if C/EBP $\beta$ -knockdown reduces the growth of xenograft tumors in vivo. Tumors were produced by injecting A549 cells subcutaneously into the dorsal area of athymic nude mice, and siNC or siC/EBP $\beta$  RNA was delivered into the tumors via electroporation. Tumor growth was monitored for seven weeks. As shown in Figure 7A, siC/EBP $\beta$  treatment markedly suppressed tumor growth by at least 50% compared with the siNC treatment. Consistent with in vitro results, immunohistochemistry analysis revealed that treatment with siC/EBP $\beta$  increased the expression of Y15-pCDK1 and Wee1 while decreasing Cdc25B expression (Figure 7B). C/EBP $\beta$ -knockdown tumors displayed lower Ki67 and higher cleaved caspase-3 expression compared with the control. These data indicate that C/EBP $\beta$  is important for tumor growth in vivo.

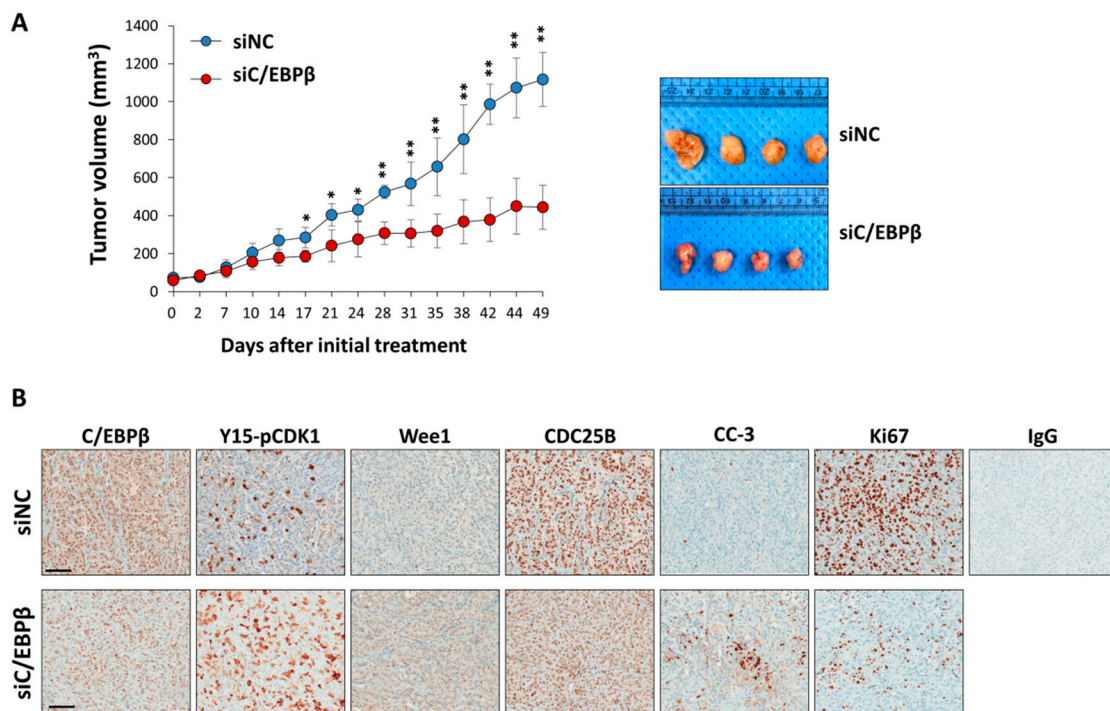


**Figure 7.** C/EBP $\beta$ -knockdown inhibits tumor growth. (A) A549 cells ( $5 \times 10^6$ ) were implanted subcutaneously into athymic nude mice. When tumor size reached 60 to 80 mm<sup>3</sup>, siNC or siC/EBP $\beta$  were delivered into the tumors via electroporation once a week for seven weeks. Tumors were measured at the indicated time and tumor volume was calculated as described in Section 2. Photos from siNC- or siC/EBP $\beta$ -treated tumors are shown. Similar results were observed in three independent experiments. Data are presented as mean  $\pm$  SD. The statistical significance was determined using the *t*-test, \*  $p < 0.05$ , \*\*  $p < 0.01$ , significantly different from siC/EBP $\beta$ -treated tumor volume. (B) Immunohistochemical staining for C/EBP $\beta$ , Y15-pCDK1, Wee1, Cdc25B, Ki67, and cleaved caspase-3 (CC-3) was conducted with paraformaldehyde-fixed, paraffin-embedded xenograft tumors. Images were captured at a magnification of 400X by using the Aperio ImageScope software. Scale bars: 100  $\mu$ m.

## 4. Discussion

Mitosis is regulated by cyclin B/CDK1 [56]. Wee1 kinase phosphorylates CDK1 at Tyr15, and dephosphorylation of this site by Cdc25 is required for the activation of CDK1 and further entry into mitosis. We showed that C/EBP $\beta$  is important for the proliferation of NSCLC cells by mediating the G<sub>2</sub>/M transition of cell cycle. C/EBP $\beta$  regulated the inhibitory phosphorylation at the Tyr15 residue of CDK1 (Figures 3 and 4). This resulted from the function of C/EBP $\beta$ , which increased the expression of Cdc25B phosphatase but inhibited the expression of Wee1 kinase at the mRNA and protein levels

(Figures 3, 4 and 5A). The mechanism of regulating Cdc25B expression by C/EBP $\beta$  does not seem to be mediated by direct transcriptional activation and is yet to be determined. C/EBP $\beta$  bound to two *WEE1* distal promoter regions,  $-4.7$  to  $-4.9$  kB and  $-4.4$  to  $-4.5$  kB, upstream of the transcription start site and repressed transcription through recruiting HDAC2 (Figure 5). These findings are summarized as a schematic diagram in Figure 8. To the best of our knowledge, this is the first report that Wee1, a key regulator of G<sub>2</sub>/M progression, is a transcriptional target of C/EBP $\beta$ . Finally, we showed that a Wee1 inhibitor, MK-1775, significantly recovered C/EBP $\beta$ -knockdown cells from the delay in the G<sub>2</sub>/M phase of the cell cycle (Figure 6). Taken together, these results indicate that C/EBP $\beta$  is a transcriptional regulator of Wee1, mitosis inhibitor protein, ultimately regulating the G<sub>2</sub>/M phase of the cell cycle progression.

Cell cycle proteins need to be tightly controlled temporally and spatially. Wee1 increases during the S and G<sub>2</sub> phase to block premature mitotic entry and then decreases during the M phase of the cell cycle [57]. Regulation of the Wee1 protein has been extensively studied and several mechanisms of modulating its kinase activity and protein levels have been demonstrated [58]. For example, Wee1 kinase activity is regulated by Akt-mediated phosphorylation on Ser642 and phosphorylated Wee1 binds to 14-3-3 $\theta$  and translocates to the cytoplasm, resulting in G<sub>2</sub>/M cell cycle progression [59]. In late G<sub>2</sub> phase, phosphorylation of Wee1 by CDK1 and polo-like kinase 1 creates a phosphodegron which targets Wee1 for SCF- $\beta$ -TrCP ubiquitin ligase-mediated proteasomal degradation [60]. However, transcriptional regulation of *WEE1* is not well known. *WEE1* transcription was shown to be repressed by direct binding of kruppel-like factor 2 (KLF2) and chromodomain helicase DNA binding protein 5 (CHD5) and activated by c-Fos/activator protein-1 (AP-1) [61–63]. Our results also demonstrated that Wee1 is downregulated by C/EBP $\beta$  via direct binding to the distal promoter and it is required for the G<sub>2</sub>/M cell cycle progression in lung cancer cells.

C/EBP $\beta$  positively regulated the proliferation of various NSCLC cells regardless of NSCLC subtypes or gene mutation status of *EGFR* or *K-RAS*, whereas it did not have a substantial effect on immortalized lung epithelial cells (Figure 2). Even if we identified Wee1 and Cdc25B as downstream players of C/EBP $\beta$  in the cell cycle regulatory role, the upstream cue, possibly altered in NSCLC, remains to be determined.

In our study, control cells after release from the thymidine double block progressed to the S phase rapidly reaching the peak levels in 2 h, and majority of them moved into the G<sub>2</sub>/M phase in another 4 h (Figure 4A,B and Figure 6A,B). However, in C/EBP $\beta$ -knockdown cells, G<sub>1</sub>/S transition was delayed and significant population of cells remained in the G<sub>0</sub>/G<sub>1</sub> phase (Figure 4A,B), suggesting that G<sub>1</sub>/S cell cycle arrest is also induced in the absence of C/EBP $\beta$ . Consistent with our observation, C/EBP $\beta$ -deficient human endometrial stromal cells underwent G<sub>1</sub>/S arrest shown by the reduction of BrdU incorporation after release from thymidine double block. In those cells, cyclin E was downregulated and thereby cyclin E-CDK2 was not functional for G<sub>1</sub>/S phase progression [64]. C/EBP $\beta$  has been shown to cooperate with E2F in activating transcription of E2F target genes involved in the G<sub>1</sub>/S transition by recruiting CBP/p300 coactivator [65].

C/EBPs are expressed in human lung epithelium and they play roles in lung development and differentiation [66]. C/EBP $\alpha$ -deficient mice displayed hyper-proliferative alveolar type II cells and a defect in alveolar architecture and suffered from respiratory distress [67,68], whereas lung phenotypes of C/EBP $\beta$  knockout mice were not specified [66]. Even if C/EBP $\beta$  is involved in the lung-specific gene expression in lung epithelial cells [69,70], it does not seem to be essential in basal lung development or differentiation, possibly due to functional redundancy with other C/EBP family members, as described in liver and mouse skin [71,72]. Rather acute lung injury is induced by lipopolysaccharide (LPS)-induced C/EBP $\beta$  mRNA [73], suggesting C/EBP $\beta$  might play a distinct role in pathological status.

Loss in the function mutations were found in acute myeloid leukemia, suggesting C/EBP $\alpha$  as potential human tumor suppressor [74]. C/EBP $\alpha$  has been reported to be down-regulated in more than 40% of human primary lung cancers [70,75], and it seems to be associated with increased

DNA methylation of *C/EBPA* promoter [76]. More recently, the oncogenic role of *C/EBPβ* has been suggested in human cancers, but how it contributes to tumorigenesis or tumor progression needs to be determined. We found that *C/EBPβ* protein is up-regulated in NSCLCs (Figure 1). Additionally, the delivery of siRNA against *C/EBPβ* into xenografted mouse tumors effectively inhibited tumor growth (Figure 7). Considering the notion that the function of *C/EBPβ* is not vital in the lung, *C/EBPβ* could be an attractive target for cancer therapy alone or in combination.

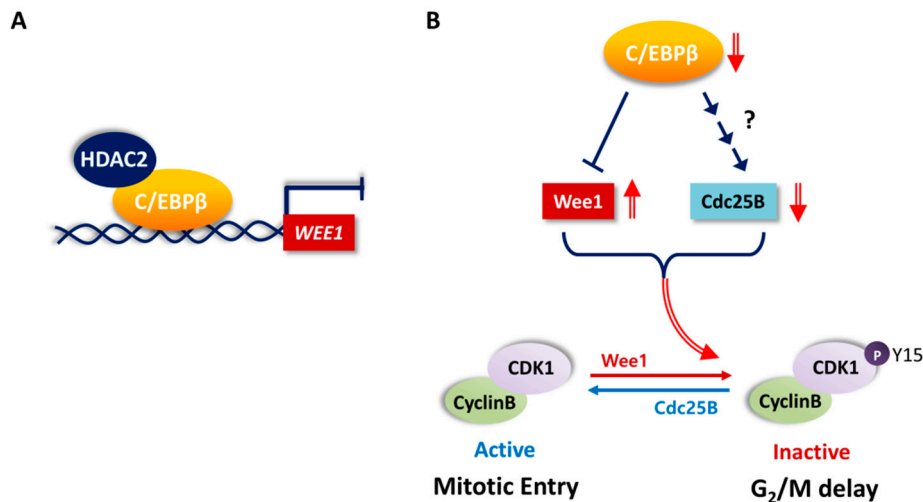


**Figure 8.** Schematic representation of the potential role of *C/EBPβ* in the  $G_2/M$  phase of cell cycle progression. (A) *C/EBPβ* represses *WEE1* transcription by directly binding to *WEE1* distal promoter regions and recruiting HDAC2. (B) *Wee1* and *Cdc25B* are key regulators of phosphorylation of tyrosine 15 residue of CDK1, which blocks mitotic entry. *C/EBPβ* activates *Cdc25B* expression via unknown mechanism but inhibits *Wee1* expression. In the absence of *C/EBPβ*, cells undergo  $G_2/M$  delay displaying increased CDK1 phosphorylation along with increased *Wee1* and decreased *Cdc25B* levels.

**Supplementary Materials:** The following are available online at <http://www.mdpi.com/2073-4409/8/2/145/s1>. Figure S1: Expression and gene alteration of *C/EBPβ* in human lung cancers. Figure S2: Overall survival (OS) and post-progression survival (PPS) of lung cancer patients. Table S1: Histological subtypes and gene mutation status of NSCLC cell lines. Figure S3: FACS analysis of mitotic cells using mitotic marker, phospho-Histone H3 (Ser10).

**Author Contributions:** Conceptualization, E.K.C. and K.Y.; Methodology, E.K.C., B.R.K., S.B.R. and K.Y.; Validation, J.H.L., E.K.C. and H.-K.Y.; Formal analysis, J.H.L., J.Y.S. and E.K.H.; Investigation, J.H.L., J.Y.S., E.K.C., H.-K.Y. and B.R.K.; Resources, B.-K.P., Y.-N.K. and S.B.R.; Writing—Original Draft Preparation, J.H.L., J.Y.S., E.K.C. and K.Y.; Writing—Review and Editing, J.H.L., J.Y.S., Y.-N.K. and K.Y.; Supervision and Funding Acquisition, K.Y.

**Funding:** This research was supported by the Basic Science Research Program through the National Research Foundation (NRF) funded by the Korean government [NRF-2016R1A2B4016618] and National Cancer Center Research Grant (1710310). And the APC was funded by [NRF-2016R1A2B4016618].

**Acknowledgments:** We would like to thank Geon Kook Lee, medical pathologist and Dongwan Hong, National Cancer Center for their comments on analysis of immunohistochemistry and public database.

**Conflicts of Interest:** The authors declare no conflicts of interest.

## References

1. Sebastian, T.; Johnson, P.F. Stop and go: Anti-proliferative and mitogenic functions of the transcription factor *C/EBPβ*. *Cell Cycle* **2006**, *5*, 953–957. [[CrossRef](#)] [[PubMed](#)]
2. Cao, Z.; Umek, R.M.; McKnight, S.L. Regulated expression of three *C/EBP* isoforms during adipose conversion of 3T3-L1 cells. *Genes Dev.* **1991**, *5*, 1538–1552. [[CrossRef](#)] [[PubMed](#)]
3. Poli, V. The role of *C/EBP* isoforms in the control of inflammatory and native immunity functions. *J. Biol. Chem.* **1998**, *273*, 29279–29282. [[CrossRef](#)] [[PubMed](#)]

4. Zahnow, C.A. CCAAT/enhancer binding proteins in normal mammary development and breast cancer. *Breast Cancer Res.* **2002**, *4*, 113–121. [[CrossRef](#)] [[PubMed](#)]
5. Ramji, D.P.; Foka, P. CCAAT/enhancer-binding proteins: Structure, function and regulation. *Biochem.J.* **2002**, *365*, 561–575. [[CrossRef](#)] [[PubMed](#)]
6. Zhu, S.; Oh, H.S.; Shim, M.; Sterneck, E.; Johnson, P.F.; Smart, R.C. C/EBPbeta modulates the early events of keratinocyte differentiation involving growth arrest and keratin 1 and keratin 10 expression. *Mol. Cell. Biol.* **1999**, *19*, 7181–7190. [[CrossRef](#)] [[PubMed](#)]
7. Guerzoni, C.; Bardini, M.; Mariani, S.A.; Ferrari-Amorotti, G.; Neviani, P.; Panno, M.L.; Zhang, Y.; Martinez, R.; Perrotti, D.; Calabretta, B. Inducible activation of CEBPB, a gene negatively regulated by BCR/ABL, inhibits proliferation and promotes differentiation of BCR/ABL-expressing cells. *Blood* **2006**, *107*, 4080–4089. [[CrossRef](#)] [[PubMed](#)]
8. Chen, X.; Liu, W.; Ambrosino, C.; Ruocco, M.R.; Poli, V.; Romani, L.; Quinto, I.; Barbieri, S.; Holmes, K.L.; Venuta, S.; et al. Impaired generation of bone marrow B lymphocytes in mice deficient in C/EBPbeta. *Blood* **1997**, *90*, 156–164. [[PubMed](#)]
9. Regalo, G.; Forster, S.; Resende, C.; Bauer, B.; Fleige, B.; Kemmner, W.; Schlag, P.M.; Meyer, T.F.; Machado, J.C.; Leutz, A. C/EBPbeta regulates homeostatic and oncogenic gastric cell proliferation. *J. Mol. Med.* **2016**, *94*, 1385–1395. [[CrossRef](#)] [[PubMed](#)]
10. Greenbaum, L.E.; Li, W.; Cressman, D.E.; Peng, Y.; Ciliberto, G.; Poli, V.; Taub, R. CCAAT enhancer-binding protein beta is required for normal hepatocyte proliferation in mice after partial hepatectomy. *J. Clin. Invest.* **1998**, *102*, 996–1007. [[CrossRef](#)] [[PubMed](#)]
11. Aguilar-Morante, D.; Cortes-Canteli, M.; Sanz-Sancristobal, M.; Santos, A.; Perez-Castillo, A. Decreased CCAAT/enhancer binding protein beta expression inhibits the growth of glioblastoma cells. *Neuroscience* **2011**, *176*, 110–119. [[CrossRef](#)] [[PubMed](#)]
12. Zhu, S.; Yoon, K.; Sterneck, E.; Johnson, P.F.; Smart, R.C. CCAAT/enhancer binding protein-beta is a mediator of keratinocyte survival and skin tumorigenesis involving oncogenic Ras signaling. *Proc. Natl. Acad. Sci. USA* **2002**, *99*, 207–212. [[CrossRef](#)] [[PubMed](#)]
13. Yoon, K.; Zhu, S.; Ewing, S.J.; Smart, R.C. Decreased survival of C/EBP beta-deficient keratinocytes is due to aberrant regulation of p53 levels and function. *Oncogene* **2007**, *26*, 360–367. [[CrossRef](#)] [[PubMed](#)]
14. Lamb, J.; Ramaswamy, S.; Ford, H.L.; Contreras, B.; Martinez, R.V.; Kittrell, F.S.; Zahnow, C.A.; Patterson, N.; Golub, T.R.; Ewen, M.E. A mechanism of cyclin D1 action encoded in the patterns of gene expression in human cancer. *Cell* **2003**, *114*, 323–334. [[CrossRef](#)]
15. Zahnow, C.A.; Younes, P.; Laucirica, R.; Rosen, J.M. Overexpression of C/EBPbeta-LIP, a naturally occurring, dominant-negative transcription factor, in human breast cancer. *J. Natl. Cancer Inst.* **1997**, *89*, 1887–1891. [[PubMed](#)]
16. Rask, K.; Thorn, M.; Ponten, F.; Kraaz, W.; Sundfeldt, K.; Hedin, L.; Enerback, S. Increased expression of the transcription factors CCAAT-enhancer binding protein-beta (C/EBPbeta) and C/EBPzeta (CHOP) correlate with invasiveness of human colorectal cancer. *Int. J. Cancer* **2000**, *86*, 337–343. [[CrossRef](#)]
17. Sundfeldt, K.; Ivarsson, K.; Carlsson, M.; Enerback, S.; Janson, P.O.; Brannstrom, M.; Hedin, L. The expression of CCAAT/enhancer binding protein (C/EBP) in the human ovary in vivo: Specific increase in C/EBPbeta during epithelial tumour progression. *Br. J. Cancer* **1999**, *79*, 1240–1248. [[CrossRef](#)] [[PubMed](#)]
18. Sankpal, N.V.; Moskaluk, C.A.; Hampton, G.M.; Powell, S.M. Overexpression of CEBPbeta correlates with decreased TFF1 in gastric cancer. *Oncogene* **2006**, *25*, 643–649. [[CrossRef](#)] [[PubMed](#)]
19. Oya, M.; Horiguchi, A.; Mizuno, R.; Marumo, K.; Murai, M. Increased activation of CCAAT/enhancer binding protein-beta correlates with the invasiveness of renal cell carcinoma. *Clin. Cancer Res.* **2003**, *9*, 1021–1027. [[PubMed](#)]
20. Regalo, G.; Canedo, P.; Suriano, G.; Resende, C.; Campos, M.L.; Oliveira, M.J.; Figueiredo, C.; Rodrigues-Pereira, P.; Blin, N.; Seruca, R.; et al. C/EBPbeta is over-expressed in gastric carcinogenesis and is associated with COX-2 expression. *J. Pathol.* **2006**, *210*, 398–404. [[CrossRef](#)] [[PubMed](#)]
21. Vermeulen, K.; Van Bockstaele, D.R.; Berneman, Z.N. The cell cycle: A review of regulation, deregulation and therapeutic targets in cancer. *Cell Proliferat.* **2003**, *36*, 131–149. [[CrossRef](#)]
22. Sherr, C.J. G1 phase progression: Cycling on cue. *Cell* **1994**, *79*, 551–555. [[CrossRef](#)]
23. Girard, F.; Strausfeld, U.; Fernandez, A.; Lamb, N.J. Cyclin A is required for the onset of DNA replication in mammalian fibroblasts. *Cell* **1991**, *67*, 1169–1179. [[CrossRef](#)]

24. Ohtsubo, M.; Theodoras, A.M.; Schumacher, J.; Roberts, J.M.; Pagano, M. Human cyclin E, a nuclear protein essential for the G1-to-S phase transition. *Mol. Cell. Biol.* **1995**, *15*, 2612–2624. [[CrossRef](#)] [[PubMed](#)]
25. King, R.W.; Jackson, P.K.; Kirschner, M.W. Mitosis in transition. *Cell* **1994**, *79*, 563–571. [[CrossRef](#)]
26. Jeffrey, P.D.; Russo, A.A.; Polyak, K.; Gibbs, E.; Hurwitz, J.; Massague, J.; Pavletich, N.P. Mechanism of CDK activation revealed by the structure of a cyclinA-CDK2 complex. *Nature* **1995**, *376*, 313–320. [[CrossRef](#)] [[PubMed](#)]
27. Lew, D.J.; Kornbluth, S. Regulatory roles of cyclin dependent kinase phosphorylation in cell cycle control. *Curr. Opin. Cell Biol.* **1996**, *8*, 795–804. [[CrossRef](#)]
28. Carnero, A.; Hannon, G.J. The INK4 family of CDK inhibitors. *Curr. Top. Microbiol. Immunol.* **1998**, *227*, 43–55. [[PubMed](#)]
29. Lee, M.H.; Reynisdottir, I.; Massague, J. Cloning of p57KIP2, a cyclin-dependent kinase inhibitor with unique domain structure and tissue distribution. *Genes Dev.* **1995**, *9*, 639–649. [[CrossRef](#)] [[PubMed](#)]
30. Polyak, K.; Lee, M.H.; Erdjument-Bromage, H.; Koff, A.; Roberts, J.M.; Tempst, P.; Massague, J. Cloning of p27Kip1, a cyclin-dependent kinase inhibitor and a potential mediator of extracellular antimitogenic signals. *Cell* **1994**, *78*, 59–66. [[CrossRef](#)]
31. Harper, J.W.; Elledge, S.J.; Keyomarsi, K.; Dynlacht, B.; Tsai, L.H.; Zhang, P.; Dobrowolski, S.; Bai, C.; Connell-Crowley, L.; Swindell, E.; et al. Inhibition of cyclin-dependent kinases by p21. *Mol. Biol. Cell* **1995**, *6*, 387–400. [[CrossRef](#)] [[PubMed](#)]
32. Bray, F.; Ferlay, J.; Soerjomataram, I.; Siegel, R.L.; Torre, L.A.; Jemal, A. Global cancer statistics 2018: GLOBOCAN estimates of incidence and mortality worldwide for 36 cancers in 185 countries. *CA Cancer J. Clin.* **2018**, *68*, 394–424. [[CrossRef](#)] [[PubMed](#)]
33. Herbst, R.S.; Morgensztern, D.; Boshoff, C. The biology and management of non-small cell lung cancer. *Nature* **2018**, *553*, 446–454. [[PubMed](#)]
34. Singhal, S.; Vachani, A.; Antin-Ozerkis, D.; Kaiser, L.R.; Albelda, S.M. Prognostic implications of cell cycle, apoptosis, and angiogenesis biomarkers in non-small cell lung cancer: A review. *Clin. Cancer Res.* **2005**, *11*, 3974–3986. [[CrossRef](#)] [[PubMed](#)]
35. Selagea, L.; Mishra, A.; Anand, M.; Ross, J.; Tucker-Burden, C.; Kong, J.; Brat, D.J. EGFR and C/EBP-beta oncogenic signaling is bidirectional in human glioma and varies with the C/EBP-beta isoform. *FASEB J.* **2016**, *30*, 4098–4108. [[CrossRef](#)] [[PubMed](#)]
36. Gavvovidis, I.; Rost, I.; Trimborn, M.; Kaiser, F.J.; Purps, J.; Wiek, C.; Hanenberg, H.; Neitzel, H.; Schindler, D. A novel MCPH1 isoform complements the defective chromosome condensation of human MCPH1-deficient cells. *PLoS ONE* **2012**, *7*, e40387. [[CrossRef](#)] [[PubMed](#)]
37. Lee, H.S.; Lee, H.K.; Kim, H.S.; Yang, H.K.; Kim, W.H. Tumour suppressor gene expression correlates with gastric cancer prognosis. *J. Pathol.* **2003**, *200*, 39–46. [[CrossRef](#)] [[PubMed](#)]
38. Gyorfy, B.; Surowiak, P.; Budczies, J.; Lanczky, A. Online survival analysis software to assess the prognostic value of biomarkers using transcriptomic data in non-small-cell lung cancer. *PLoS ONE* **2013**, *8*, e82241. [[CrossRef](#)] [[PubMed](#)]
39. Sutherland, K.D.; Berns, A. Cell of origin of lung cancer. *Mol. Oncol.* **2010**, *4*, 397–403. [[CrossRef](#)] [[PubMed](#)]
40. Blanco, R.; Iwakawa, R.; Tang, M.; Kohno, T.; Angulo, B.; Pio, R.; Montuenga, L.M.; Minna, J.D.; Yokota, J.; Sanchez-Cespedes, M. A gene-alteration profile of human lung cancer cell lines. *Hum. Mutat.* **2009**, *30*, 1199–1206. [[CrossRef](#)] [[PubMed](#)]
41. Den Dunnen, J.T.; Antonarakis, S.E. Mutation nomenclature extensions and suggestions to describe complex mutations: A discussion. *Hum. Mutat.* **2000**, *15*, 7–12. [[CrossRef](#)]
42. Forbes, S.; Clements, J.; Dawson, E.; Bamford, S.; Webb, T.; Dogan, A.; Flanagan, A.; Teague, J.; Wooster, R.; Futreal, P.A.; et al. COSMIC 2005. *Br. J. Cancer* **2006**, *94*, 318–322. [[CrossRef](#)] [[PubMed](#)]
43. Wistuba, II.; Bryant, D.; Behrens, C.; Milchgrub, S.; Virmani, A.K.; Ashfaq, R.; Minna, J.D.; Gazdar, A.F. Comparison of features of human lung cancer cell lines and their corresponding tumors. *Clin. Cancer Res.* **1999**, *5*, 991–1000. [[PubMed](#)]
44. Yamamoto, H.; Shigematsu, H.; Nomura, M.; Lockwood, W.W.; Sato, M.; Okumura, N.; Soh, J.; Suzuki, M.; Wistuba, II.; Fong, K.M.; Lee, H.; et al. PIK3CA mutations and copy number gains in human lung cancers. *Cancer Res.* **2008**, *68*, 6913–6921. [[CrossRef](#)] [[PubMed](#)]
45. Obaya, A.J.; Sedivy, J.M. Regulation of cyclin-Cdk activity in mammalian cells. *Cell. Mol. Life Sci.* **2002**, *59*, 126–142. [[CrossRef](#)] [[PubMed](#)]

46. O'Farrell, P.H. Triggering the all-or-nothing switch into mitosis. *Trends Cell Biol.* **2001**, *11*, 512–519. [[CrossRef](#)]
47. Parker, L.L.; Piwnica-Worms, H. Inactivation of the p34cdc2-cyclin B complex by the human WEE1 tyrosine kinase. *Science* **1992**, *257*, 1955–1957. [[CrossRef](#)] [[PubMed](#)]
48. Mueller, P.R.; Coleman, T.R.; Kumagai, A.; Dunphy, W.G. Myt1: A membrane-associated inhibitory kinase that phosphorylates Cdc2 on both threonine-14 and tyrosine-15. *Science* **1995**, *270*, 86–90. [[CrossRef](#)] [[PubMed](#)]
49. Donzelli, M.; Draetta, G.F. Regulating mammalian checkpoints through Cdc25 inactivation. *EMBO Rep.* **2003**, *4*, 671–677. [[CrossRef](#)] [[PubMed](#)]
50. Dunphy, W.G.; Kumagai, A. The cdc25 protein contains an intrinsic phosphatase activity. *Cell* **1991**, *67*, 189–196. [[CrossRef](#)]
51. Glotzer, M. Mitosis: Don't get mad, get even. *Curr. Biol.* **1996**, *6*, 1592–1594. [[CrossRef](#)]
52. Meraldi, P.; Draviam, V.M.; Sorger, P.K. Timing and checkpoints in the regulation of mitotic progression. *Dev. Cell* **2004**, *7*, 45–60. [[CrossRef](#)] [[PubMed](#)]
53. Hendzel, M.J.; Wei, Y.; Mancini, M.A.; Van Hooser, A.; Ranalli, T.; Brinkley, B.R.; Bazett-Jones, D.P.; Allis, C.D. Mitosis-specific phosphorylation of histone H3 initiates primarily within pericentromeric heterochromatin during G2 and spreads in an ordered fashion coincident with mitotic chromosome condensation. *Chromosoma* **1997**, *106*, 348–360. [[CrossRef](#)] [[PubMed](#)]
54. Kent, W.J.; Sugnet, C.W.; Furey, T.S.; Roskin, K.M.; Pringle, T.H.; Zahler, A.M.; Haussler, D. The human genome browser at UCSC. *Genome Res.* **2002**, *12*, 996–1006. [[CrossRef](#)] [[PubMed](#)]
55. Wang, G.L.; Salisbury, E.; Shi, X.; Timchenko, L.; Medrano, E.E.; Timchenko, N.A. HDAC1 promotes liver proliferation in young mice via interactions with C/EBPbeta. *J. Biol. Chem.* **2008**, *283*, 26179–26187. [[CrossRef](#)] [[PubMed](#)]
56. Castedo, M.; Perfettini, J.L.; Roumier, T.; Kroemer, G. Cyclin-dependent kinase-1: Linking apoptosis to cell cycle and mitotic catastrophe. *Cell Death Differ.* **2002**, *9*, 1287–1293. [[CrossRef](#)] [[PubMed](#)]
57. McGowan, C.H.; Russell, P. Cell cycle regulation of human WEE1. *EMBO J.* **1995**, *14*, 2166–2175. [[CrossRef](#)] [[PubMed](#)]
58. Perry, J.A.; Kornbluth, S. Cdc25 and Wee1: Analogous opposites? *Cell Div.* **2007**, *2*, 12. [[CrossRef](#)] [[PubMed](#)]
59. Katayama, K.; Fujita, N.; Tsuruo, T. Akt/protein kinase B-dependent phosphorylation and inactivation of WEE1Hu promote cell cycle progression at G2/M transition. *Mol. Cell. Biol.* **2005**, *25*, 5725–5737. [[CrossRef](#)] [[PubMed](#)]
60. Watanabe, N.; Arai, H.; Nishihara, Y.; Taniguchi, M.; Watanabe, N.; Hunter, T.; Osada, H. M-phase kinases induce phospho-dependent ubiquitination of somatic Wee1 by SCFbeta-TrCP. *Proc. Natl. Acad. Sci. USA* **2004**, *101*, 4419–4424. [[CrossRef](#)] [[PubMed](#)]
61. Wang, F.; Zhu, Y.; Huang, Y.; McAvoy, S.; Johnson, W.B.; Cheung, T.H.; Chung, T.K.; Lo, K.W.; Yim, S.F.; Yu, M.M.; et al. Transcriptional repression of WEE1 by Kruppel-like factor 2 is involved in DNA damage-induced apoptosis. *Oncogene* **2005**, *24*, 3875–3885. [[CrossRef](#)] [[PubMed](#)]
62. Kawasaki, H.; Komai, K.; Ouyang, Z.; Murata, M.; Hikasa, M.; Ohgiri, M.; Shiozawa, S. c-Fos/activator protein-1 transactivates wee1 kinase at G(1)/S to inhibit premature mitosis in antigen-specific Th1 cells. *EMBO J.* **2001**, *20*, 4618–4627. [[CrossRef](#)] [[PubMed](#)]
63. Quan, J.; Adelmant, G.; Marto, J.A.; Look, A.T.; Yusufzai, T. The chromatin remodeling factor CHD5 is a transcriptional repressor of WEE1. *PLoS ONE* **2014**, *9*, e108066. [[CrossRef](#)] [[PubMed](#)]
64. Wang, W.; Taylor, R.N.; Bagchi, I.C.; Bagchi, M.K. Regulation of human endometrial stromal proliferation and differentiation by C/EBPbeta involves cyclin E-cdk2 and STAT3. *Mol. Endocrinol.* **2012**, *26*, 2016–2030. [[CrossRef](#)] [[PubMed](#)]
65. Wang, H.; Larris, B.; Peiris, T.H.; Zhang, L.; Le Lay, J.; Gao, Y.; Greenbaum, L.E. C/EBPbeta activates E2F-regulated genes in vivo via recruitment of the coactivator CREB-binding protein/P300. *J. Biol. Chem.* **2007**, *282*, 24679–24688. [[CrossRef](#)] [[PubMed](#)]
66. Cassel, T.N.; Nord, M. C/EBP transcription factors in the lung epithelium. *Am. J. Physiol. Lung Cell. Mol. Physiol.* **2003**, *285*, L773–L781. [[CrossRef](#)] [[PubMed](#)]
67. Sugahara, K.; Iyama, K.I.; Kimura, T.; Sano, K.; Darlington, G.J.; Akiba, T.; Takiguchi, M. Mice lacking CCAAt/enhancer-binding protein-alpha show hyperproliferation of alveolar type II cells and increased surfactant protein mRNAs. *Cell Tissue Res.* **2001**, *306*, 57–63. [[CrossRef](#)] [[PubMed](#)]

68. Flodby, P.; Barlow, C.; Kylefjord, H.; Ahrlund-Richter, L.; Xanthopoulos, K.G. Increased hepatic cell proliferation and lung abnormalities in mice deficient in CCAAT/enhancer binding protein alpha. *J. Biol. Chem.* **1996**, *271*, 24753–24760. [[CrossRef](#)] [[PubMed](#)]
69. Park, Y.; Kemper, B. The CYP2B1 proximal promoter contains a functional C/EBP regulatory element. *DNA Cell Biol.* **1996**, *15*, 693–701. [[CrossRef](#)] [[PubMed](#)]
70. He, Y.; Crouch, E. Surfactant protein D gene regulation. Interactions among the conserved CCAAT/enhancer-binding protein elements. *J. Biol. Chem.* **2002**, *277*, 19530–19537. [[CrossRef](#)] [[PubMed](#)]
71. Chen, S.S.; Chen, J.F.; Johnson, P.F.; Muppala, V.; Lee, Y.H. C/EBPbeta, when expressed from the C/ebpalpha gene locus, can functionally replace C/EBPalpha in liver but not in adipose tissue. *Mol. Cell. Biol.* **2000**, *20*, 7292–7299. [[CrossRef](#)] [[PubMed](#)]
72. House, J.S.; Zhu, S.; Ranjan, R.; Linder, K.; Smart, R.C. C/EBPalpha and C/EBPbeta are required for Sebocyte differentiation and stratified squamous differentiation in adult mouse skin. *PLoS ONE* **2010**, *5*, e9837. [[CrossRef](#)] [[PubMed](#)]
73. Sugahara, K.; Sadohara, T.; Sugita, M.; Iyama, K.; Takiguchi, M. Differential expression of CCAAT enhancer binding protein family in rat alveolar epithelial cell proliferation and in acute lung injury. *Cell Tissue Res.* **1999**, *297*, 261–270. [[CrossRef](#)] [[PubMed](#)]
74. Gombart, A.F.; Hofmann, W.K.; Kawano, S.; Takeuchi, S.; Krug, U.; Kwok, S.H.; Larsen, R.J.; Asou, H.; Miller, C.W.; Hoelzer, D.; et al. Mutations in the gene encoding the transcription factor CCAAT/enhancer binding protein alpha in myelodysplastic syndromes and acute myeloid leukemias. *Blood* **2002**, *99*, 1332–1340. [[CrossRef](#)] [[PubMed](#)]
75. Halmos, B.; Huettner, C.S.; Kocher, O.; Ferenczi, K.; Karp, D.D.; Tenen, D.G. Down-regulation and antiproliferative role of C/EBPalpha in lung cancer. *Cancer Res.* **2002**, *62*, 528–534. [[PubMed](#)]
76. Tada, Y.; Brena, R.M.; Hackanson, B.; Morrison, C.; Otterson, G.A.; Plass, C. Epigenetic modulation of tumor suppressor CCAAT/enhancer binding protein alpha activity in lung cancer. *J. Natl. Cancer Inst.* **2006**, *98*, 396–406. [[CrossRef](#)] [[PubMed](#)]



© 2019 by the authors. Licensee MDPI, Basel, Switzerland. This article is an open access article distributed under the terms and conditions of the Creative Commons Attribution (CC BY) license (<http://creativecommons.org/licenses/by/4.0/>).